



HAL
open science

Impact of rare earth element clusters on the excited state lifetime evolution under irradiation in oxide glasses

Vera Pukhkaya, Philippe Goldner, Alban Ferrier, Nadège Ollier

► To cite this version:

Vera Pukhkaya, Philippe Goldner, Alban Ferrier, Nadège Ollier. Impact of rare earth element clusters on the excited state lifetime evolution under irradiation in oxide glasses. *Optics Express*, 2015, 23 (3), pp.3270-3281. 10.1364/OE.23.003270 . hal-01275486

HAL Id: hal-01275486

<https://hal.sorbonne-universite.fr/hal-01275486>

Submitted on 17 Feb 2016

HAL is a multi-disciplinary open access archive for the deposit and dissemination of scientific research documents, whether they are published or not. The documents may come from teaching and research institutions in France or abroad, or from public or private research centers.

L'archive ouverte pluridisciplinaire **HAL**, est destinée au dépôt et à la diffusion de documents scientifiques de niveau recherche, publiés ou non, émanant des établissements d'enseignement et de recherche français ou étrangers, des laboratoires publics ou privés.



Distributed under a Creative Commons Attribution 4.0 International License

Impact of rare earth element clusters on the excited state lifetime evolution under irradiation in oxide glasses

Vera Pukhkaya¹, Philippe Goldner,² Alban Ferrier^{2,3} and Nadège Ollier^{1*}

¹Laboratoire des Solides Irradiés, UMR 7642 CEA-CNRS-Ecole Polytechnique, Palaiseau, France

²PSL Research University, Chimie ParisTech - CNRS, Institut de Recherche de Chimie Paris, 75005, Paris, France

³Sorbonne Universités, UPMC Univ Paris 06, 75005, Paris, France

*nadege.ollier@polytechnique.edu

Abstract: Rare earth doped active glasses and fibers can be exposed to ionizing radiations in space and nuclear applications. In this work, we analyze the evolution of $^2F_{5/2}$ excited state lifetime in Yb^{3+} ions in irradiated aluminosilicate glasses by electrons and γ rays. It is found that the variation of lifetimes depends on the Yb^{3+} clusters content of the glasses for irradiation doses in the $10^2 - 1.5 \cdot 10^9$ Gy range. In particular, glasses with high clustering show a smaller decrease in lifetime with increasing radiation dose. This behavior is well correlated to the variation in paramagnetic defects concentration determined by electron paramagnetic resonance. This effect is also observed in Yb^{3+} doped phosphate and Er^{3+} doped aluminosilicate glasses, inferring that clustering plays an important role in irradiation induced quenching.

©2015 Optical Society of America

OCIS codes: (140.3615) Lasers, ytterbium; (160.5690) Rare-earth-doped materials; (160.2750) Glass and other amorphous materials; (260.3800) Luminescence; (350.5610) Radiation.

References and links

1. P. Barua, E. H. Sekiya, K. Saito, and A. J. Ikushima, "Influence of Yb^{3+} ion concentration on the spectroscopic properties of silica glass," *J. Non-Cryst. Solids* **354**(42-44), 4760–4764 (2008).
2. B. Schaudel, P. Goldner, M. Prassas, and F. Auzel, "Cooperative luminescence as a probe of clustering in Yb^{3+} doped glasses," *J. Alloy. Comp.* **300–301**, 443–449 (2000).
3. P. Goldner, B. Schaudel, and M. Prassas, "Dependence of cooperative luminescence intensity on Yb^{3+} spatial distribution in crystals and glasses," *Phys. Rev. B* **65**(5), 054103 (2002).
4. S. Girard, M. Vivona, A. Laurent, B. Cadier, C. Marcandella, T. Robin, E. Pinsard, A. Boukenter, and Y. Ouerdane, "Radiation hardening techniques for Er/Yb doped optical fibers and amplifiers for space application," *Opt. Express* **20**(8), 8457–8465 (2012).
5. N. Ollier, J.-L. Doualan, V. Pukhkaya, T. Charpentier, R. Moncorgé, and S. Sen, "Evolution of Yb^{3+} environment and luminescence properties under ionizing irradiation in aluminoborosilicate glasses," *J. Non-Cryst. Solids* **357**(3), 1037–1043 (2011).
6. B. Tortech, Ph. D. dissertation, Saint-Etienne, (2008).
7. B. Tortech, Y. Ouerdane, S. Girard, J.-P. Meunier, A. Boukenter, T. Robin, B. Cadier, and P. Crochet, "Radiation effects on Yb- and Er/Yb-doped optical fibers: a micro-luminescence study," *J. Non-Cryst. Solids* **355**(18-21), 1085–1088 (2009).
8. A. Polman and J. M. Poate, "Ion irradiation damage in Er-doped silica probed by the Er^{3+} luminescence lifetime at 1.535 μm ," *J. Appl. Phys.* **73**(4), 1669–1674 (1993).
9. V. Pukhkaya, T. Charpentier, and N. Ollier, "Study of formation and sequential relaxation of paramagnetic point defects in electron-irradiated Na-aluminosilicate glasses: influence of Yb," *J. Non-Cryst. Solids* **364**, 1–8 (2013).
10. B. Schaudel Ph. D dissertation, Paris 6, (2000)
11. S. Sen, R. Rakhmatullin, R. Gubaidullin, and A. Pöppl, "Direct spectroscopic observation of the atomic-scale mechanisms of clustering and homogenization of rare-earth dopant ions in vitreous silica," *Phys. Rev. B* **74**(10), 100201 (2006).
12. N. Ollier, R. Planchais, and B. Boizot, "EPR study of Yb-doped irradiated glasses" *Nucl. Instr. and Meth. in Phys. Res. B*, **266**, 2854–2858, (2008).
13. L. Skuja, "Optically active oxygen-deficiency-related centers in amorphous silica dioxide," *J. Non-Cryst. Solids* **239**(1-3), 16–48 (1998).

1. Introduction

Yb³⁺ ion is an essential dopant in glasses and fibers for IR-lasers due to its highly-efficient emission at ~1 μm. Owing to its unusual energy level scheme with only two manifolds separated by about 10000 cm⁻¹, Yb³⁺ offers interesting spectroscopic properties for optical applications such as absence of excited state absorption and relatively long emission lifetime. The lifetime of Yb³⁺ excited state ²F_{5/2} is an important spectroscopic parameter because it determines the laser pump saturation intensity $I_{\text{sat}} \sim 1/\tau_{\text{IR}}$ which should be as low as possible [1].

To increase the IR-laser gain, Yb³⁺ concentration can be increased but results in the formation of clusters, especially in pure SiO₂ glasses where the network rigidity is not suitable to host a high content of rare earth ions. In glasses containing modifier ions, the local environment of Yb³⁺ ions is defined preferentially by Non-Bridging Oxygens. Their concentration impacts the Yb clusters content in oxide glasses as was demonstrated in aluminosilicate, phosphate and aluminoborosilicate glasses [2, 3].

Active fibers such as Yb³⁺ or Er³⁺ doped ones can be exposed to ionizing radiations in nuclear or space applications [4]. Besides quantifying the Radiation Induced Absorption (RIA) and analyzing the corresponding point defects, it is also necessary to estimate the influence of ionizing radiations on rare earth element spectroscopic properties in these fibers. Only a few papers have reported such studies up to now. It has been shown that ionizing radiations (electron, γ rays) can affect Yb³⁺ spectroscopic properties in aluminoborosilicate glasses such as the ²F_{5/2} excited state lifetime and the cooperative emission intensity [5]. This was correlated to the formation of hole centers type defect under irradiation, in this case, Non-Bridging Oxygen Hole Centers (NBOHC) [5]. In Er-doped fibers, a similar decrease of ⁴I_{13/2} lifetime has been observed under γ-irradiation [6, 7] and ion radiation [8]. This was attributed to non-radiative energy transfers from the ⁴I_{13/2} level to radiation-induced point defects [6, 7].

In the present study, we investigate the evolution of Yb³⁺ excited state lifetime under ionizing radiations (electrons, γ rays) for a broad dose range (10²-10⁹ Gy) in a series of aluminosilicate glasses. The composition of these glasses was chosen to study the influence of Yb³⁺ clustering on spectroscopic changes. This was motivated by our previous observation of Yb³⁺ clustering impact on the thermal recovery of radiation induced paramagnetic point defects [9]. Here, we show that Yb³⁺ excited state lifetime decreases at a lower rate as a function of the irradiation dose in glasses with high clusters amount. A good agreement is also found with the variation of the defect concentration in these glasses. The same excited state lifetime evolution is also observed in Yb³⁺ doped phosphate glasses and Er³⁺ doped aluminosilicate glasses, suggesting that this behavior is independent on the particular rare earth-glass combination.

2. Experimental details

Four Yb-doped and two Er-containing aluminosilicate glass compositions were synthesized. For that, appropriate amounts of dried powders of SiO₂, Al₂O₃, Na₂CO₃, Yb₂O₃ or Er₂O₃ were mixed thoroughly to obtain a well-homogenized powder and slowly heated (during 10 hours) in a Pt-Au crucible from room temperature up to 1600°C (melting temperature) in a furnace under air during 4 hours. Slow heating facilitated the CO₂ release process taking place at ~800°C. In addition, it promoted higher homogeneity of the melt. Afterwards, glasses were quenched at room temperature and annealed at 580°C (below T_g) in order to reduce the residual thermal stresses. The nominal aluminosilicate glass compositions are presented in Table 1. Samples are labeled according to the Aluminum Saturation Index (ASI = Al/Na), which characterizes the Non-Bridging Oxygen concentration. Actual glass compositions were

determined with microprobe analysis giving <1 mol. % of error compared to nominal compositions.

Phosphate glass samples were prepared starting from $\text{NH}_4\text{H}_2\text{PO}_4$, MgO , Na_2CO_3 and Yb_2O_3 (5 wt. %). The initial powders were mixed and melted in a silica crucible and then slowly heated from room temperature up to 900°C . As in the case of aluminosilicate glasses, slow heating favored CO_2 release and homogenization. The melted glass was quenched rapidly into a Pt-Au crucible on an electric plate at 300°C to avoid a high cooling rate, and immediately annealed at 350°C to reduce residual thermal stresses. The nominal phosphate glass compositions are presented in Table 2.

Table 1. Nominal Yb^{3+} and Er^{3+} -doped Aluminosilicate Glass Compositions

Sample name	SiO_2 , mol. %	Al_2O_3 , mol. %	Na_2O , mol. %	ASI Al/Na	
ASI03_Yb5	74	6	20	0.3	
ASI06_Yb5	68	12	20	0.6	
ASI09_Yb5	62	18	20	0.9	+ 5 wt. % Yb_2O_3
ASI11_Yb5	58	22	20	1.1	
ASI09_Yb05	62	18	20	0.9	+ 0.5 wt. % Yb_2O_3
ASI09_Yb8	62	18	20	0.9	+ 8 wt. % Yb_2O_3
ASI03_Er	74	6	20	0.3	+ 0.5 wt. % Er_2O_3
ASI09_Er	62	18	20	0.9	+ 0.5 wt. % Er_2O_3

Bulk glass samples ($5 \times 5 \text{ mm}^2$, 500-700 μm thickness) were continuously irradiated at SIRIUS electron accelerator (Laboratoire des Solides Irradiés, Palaiseau, France) with the 2.5 MeV electron beam with a dose rate close to 25 MGy/h. The sample holder was maintained around 40°C with a water-cooling system. The achieved integrated doses were 10^5 , 10^6 , $3 \cdot 10^6$, 10^7 , 10^8 and $1.5 \cdot 10^9$ Gy. Samples were also irradiated with γ -rays of 1.25 MeV from Co^{60} source in “Centre National des Sciences et Technologies Nucléaires” in Tunisia (CNSTN). The dose rate in this case was 5.64 kGy/h. The achieved doses were 10^4 , 10^5 , 10^6 and $3 \cdot 10^6$ Gy. Two lower doses 100 Gy and 1000 Gy were achieved with γ -rays of 1.25 MeV from Co^{60} source in “Institut de Radioprotection et de Sûreté Nucléaire” (IRSN, Fontenay-aux-Roses, France). The dose rate was 2 Gy/min. The error bar on the radiation dose after electron irradiation is considered as 10% because of the backscattered electrons that were not taken into account in the dose calculation”. Concerning gamma rays irradiation, at 100 Gy the error is 5.5%.

Table 2. Nominal Yb^{3+} -doped Phosphate Glass Compositions

Sample name	P_2O_5 , mol. %	MgO , mol. %	Na_2O , mol. %	
MP50	50	16.7	33.3	
PIP45	45.4	18.2	36.4	+ 5 wt.% Yb_2O_3
PIP40	40	20	40	

Yb^{3+} emission ${}^2\text{F}_{5/2} \rightarrow {}^2\text{F}_{7/2}$ in the IR-region was recorded on a HORIBA Jobin Yvon spectrofluorimeter under Xe lamp excitation at 975 nm with a 1200 gr/mm grating and a RG-830 filter. The lifetime of Yb^{3+} excited state ${}^2\text{F}_{5/2}$ was measured at 1000 nm with a time resolution of 100 μs . The lifetime of $\text{Er}^{3+} {}^4\text{I}_{13/2}$ excited state was measured using pulsed laser excitation at 975 nm (Ekspla optical parametric oscillator NT342B) and detection by an InGaAs detector. Yb^{3+} cooperative luminescence was excited at 975 nm by a laser diode, dispersed by a Jobin-Yvon H25 spectrometer and detected by a photon counting photomultiplier tube. In order to perform accurate cooperative luminescence measurements, the samples were grounded into powders of well-controlled particle size in the range 100-125 μm [2].

Electron Paramagnetic Resonance (EPR) experiments were carried out on a Bruker X-band EMX spectrometer. Paramagnetic point defects were analyzed at room temperature and Yb^{3+} signal was recorded at 4K. The microwave frequency was 9.8 GHz. Spectra were

normalized by attenuator gain and sample mass to allow quantitative comparisons. Radiation-induced point defects were also analyzed by time-resolved photoluminescence at room temperature. We used a frequency-doubled pulsed Nd:YAG laser for excitation and a Shamrock SR-303i spectrometer and an ANDOR ICCD camera for detection. The delay was 500 ns and the gate width was 100 μ s.

3. Results and discussion

3.1 Yb^{3+} doped aluminosilicate glasses

3.1.1 Optical and EPR spectroscopy of non-irradiated samples

The lifetimes τ_{IR} of ${}^2\text{F}_{5/2}$ Yb^{3+} excited state in non-irradiated aluminosilicate glasses are displayed in Table 3. Although the concentration of Yb^{3+} was maintained at 5 wt. % of Yb_2O_3 , we observed that τ_{IR} decreased from 2.14 ms in ASI03_Yb5 glass to 0.94 ms in ASI11_Yb5 glass. We attribute this to changes in Yb^{3+} environment in the different glasses, resulting in variations of the ${}^2\text{F}_{5/2} \rightarrow {}^2\text{F}_{7/2}$ transition oscillator strength [10].

Table 3. $\text{Yb}^{3+} {}^2\text{F}_{5/2}$ Lifetimes in Non-irradiated Aluminosilicate Glasses

Glass sample	${}^2\text{F}_{5/2}$ lifetime (ms)
ASI03_Yb5	2.14
ASI06_Yb5	1.97
ASI09_Yb5	1.15
ASI11_Yb5	0.94

Yb^{3+} environment changes are also clearly seen in the normalized emission spectra shown in Fig. 1. In particular, the peak located at 1006 nm in ASI03_Yb5 and ASI06_Yb5 shifts to 1027 nm in ASI09_Yb5 and ASI11_Yb5 glasses. This could reflect a larger Stark splitting in the latter glasses due to a stronger crystal field. These changes in Yb^{3+} environment were confirmed by EPR spectroscopy (see below).

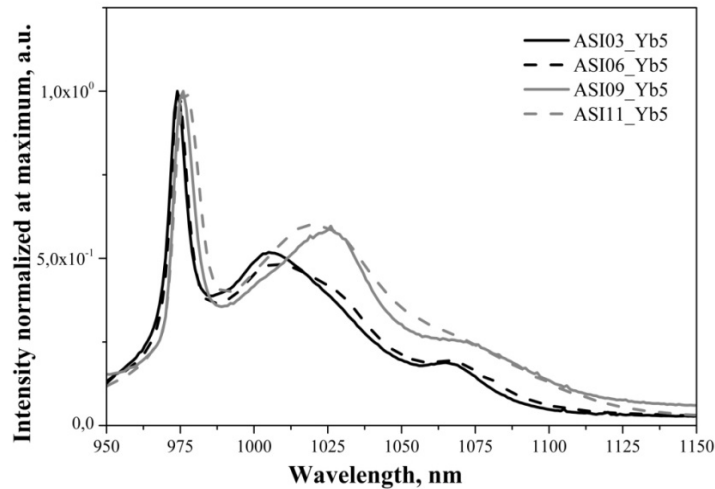


Fig. 1. Normalized Yb^{3+} emission spectra in non-irradiated Yb^{3+} doped aluminosilicate glasses under 975 nm excitation.

Yb^{3+} clustering was probed by cooperative luminescence [2]. Corresponding spectra for non-irradiated glasses are shown in Fig. 2. Spectra were normalized by the factor $(\alpha_{\text{D}} * \tau_{\text{IR}})^2$, where α_{D} is the absorption coefficient calculated by integrating the product of the absorption spectrum of the sample by the emission spectrum of the diode (normalized at maximum). Since excitation absorption was low in the powder geometry, the cooperative emission probability, which reflects Yb^{3+} cluster concentration, was proportional to the area under the

normalized cooperative emission spectra [3]. The cooperative emission probability increases strongly from ASI03_Yb5 glass to ASI11_Yb5 (Fig. 2) and the glass series can be divided into two groups: ASI03_Yb5-ASI06_Yb5 (low Yb³⁺ cluster amount) and ASI09_Yb5-ASI11_Yb5 (high Yb³⁺ cluster amount). The high clustering in ASI09 and ASI11 glass compositions can be explained by a lower amount of NBO due to an increasing Al³⁺ content that must be compensated by Na⁺ ions [2]. We checked by MAS NMR of ²⁷Al the fourfold coordination of Al³⁺ in those glasses [9] in order to exclude any modifications of Al³⁺ coordination number.

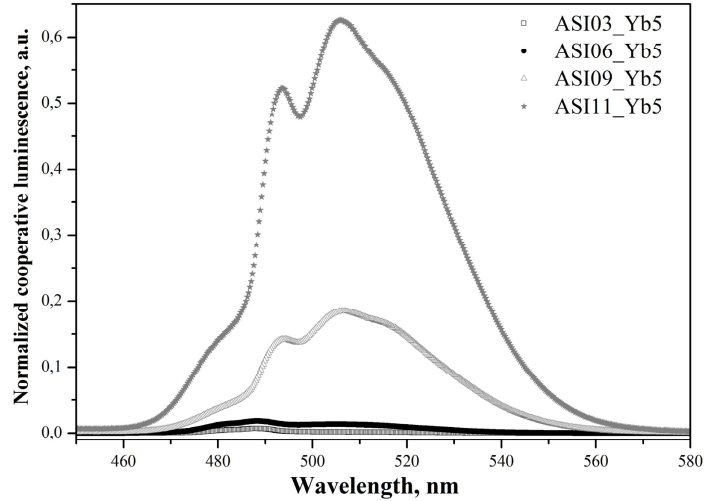


Fig. 2. Normalized cooperative luminescence spectra of non-irradiated Yb-doped aluminosilicate glasses.

To further probe Yb³⁺ environment and clustering, EPR spectra were recorded at 4K (Fig. 3). The broad line in the whole range of magnetic field corresponds to well-diluted Yb³⁺ ions in glass [5, 11, 12]. In ASI09_Yb5 and ASI11_Yb5 glasses, the EPR signal is much lower despite the same amount of Yb³⁺ in all four glasses (Fig. 3, inset). This decrease indicates that part of Yb³⁺ ions is not detected, probably because of too short spin relaxation time T_1 . This can be due to the formation of Yb³⁺ ion clusters [11], in agreement with the cooperative luminescence results. Besides, in both glasses, a shoulder at $g = 12.8$ can be seen, which we assign to Yb³⁺ clusters [16]. Indeed, the theoretical g -value for isolated Yb³⁺ ions does not exceed $2\Lambda \cdot M$ where M is the maximum of the projection of the total angular momentum and Λ is the Landé factor. The ground multiplet of Yb³⁺ is $^2F_{7/2}$, corresponding to $\Lambda = 8/7$ and $M = 7/2$. Thus, $g_{\max} \sim 8$ for isolated Yb³⁺ ions [11], suggesting that the $g = 12.8$ shoulder corresponds to clusters.

Yb³⁺ EPR spectra were analyzed in more details by assuming an axial site symmetry. Determining the exact parameters of the g -tensor is difficult in glasses because of inhomogeneous broadening. The value of g_{\perp} is estimated to 3.2 in ASI03_Yb5 and ASI06_Yb5 and 4.1 in ASI09_Yb5 and ASI11_Yb5 glasses. We did not perform simulations to obtain g_{\parallel} parameters but we estimate $g_{\parallel} \sim 1.3$ -1.4 in ASI03_Yb5 and ASI06_Yb5 and $g_{\parallel} \sim 1.1$ in ASI09_Yb5 and ASI11_Yb5. The variation in g_{\perp} with glass composition is in agreement with the emission spectra and reflects different environments for Yb³⁺ ions in low and high ASI index glasses. It should also be noted that the g_{\perp} factors obtained in Yb-doped aluminoborosilicate (ABS) glasses with low clustering content were in the range 3.17 to 3.32 [12], close to the values found here for ASI03_Yb5 and ASI06_Yb5, in which clustering is low too.

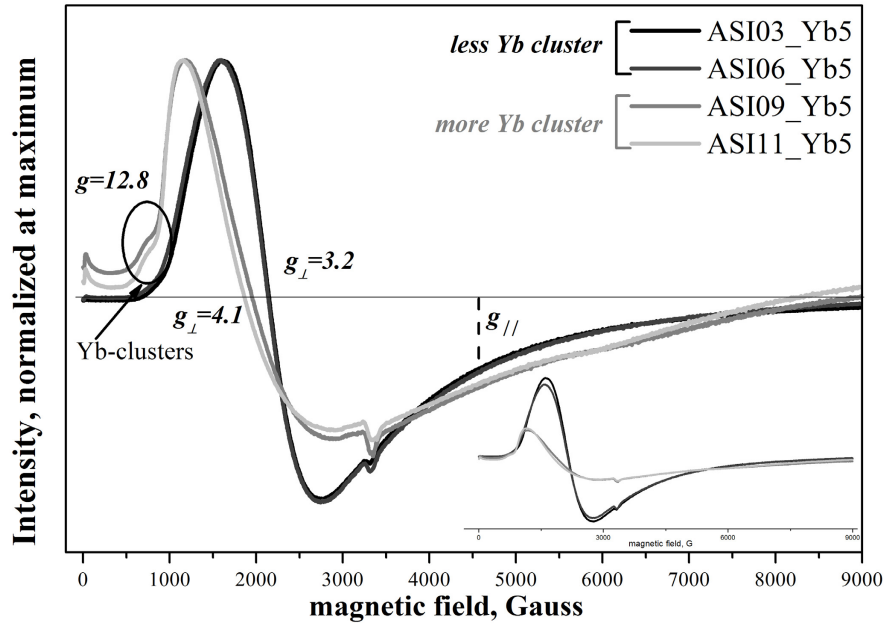


Fig. 3. EPR spectra normalized at maximum signal of non-irradiated Yb-doped aluminosilicate glasses ($T = 4\text{K}$). Inset: normalization by mass and gain only.

3.1.2 Evolution of $\text{Yb}^{3+} {}^2\text{F}_{5/2}$ lifetime under irradiation in aluminosilicate glasses

First, we studied the evolution of lifetimes after irradiation for delays up to 4 months. Despite irradiation, all fluorescence decays were well fitted by a single exponential. Figure 4 displays the obtained τ_{IR} values in irradiated glasses at 10^5 Gy at different times after irradiation. The values before irradiation are labeled by larger symbols. In all samples, irradiation results in a clear decrease (40-50%) of the ${}^2\text{F}_{5/2}$ lifetime. Then, for glasses ASI09_Yb5 and ASI11_Yb5 there is almost no variation of τ_{IR} for delays up to 4 months. In opposition, for glasses ASI03_Yb5 and ASI06_Yb5, one can observe a slight increase of the τ_{IR} . In all glasses, the lifetime of Yb^{3+} excited state ${}^2\text{F}_{5/2}$ did not reach its pre-irradiation value on the time scale investigated.

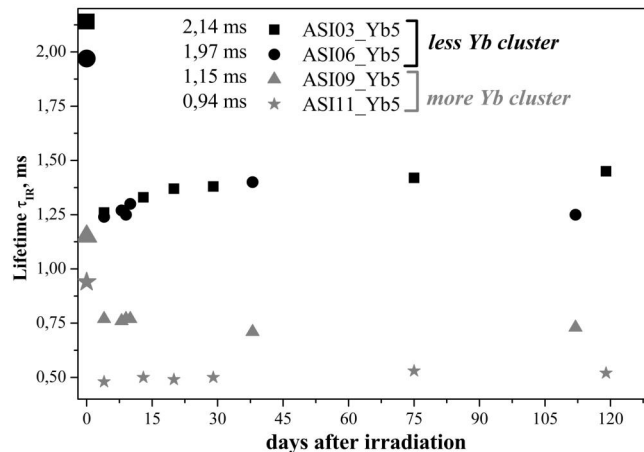


Fig. 4. ${}^2\text{F}_{5/2}$ lifetimes of Yb^{3+} excited state recorded at different times after electron irradiation (10^5 Gy dose). The non-irradiated glasses are shown with larger symbols.

This behavior can be understood by considering that the ${}^2F_{5/2}$ level is quenched by the defects induced by the irradiation. Indeed, the concentration of paramagnetic point defects induced by irradiation decreases with time, with a slower rate in glasses with higher Yb^{3+} clustering [9]. This is explained by the ability of clustered Yb^{3+} ions to efficiently trap charges under a stable form during the irradiation process. As a consequence, point defects thermal recovery is slowed down, as its τ_{IR} increase.

We also analyzed the dose effect on τ_{IR} lifetime after 6 months to reach stable values. Figure 5 displays τ_{IR} as a function of $\lg(\text{dose})$ obtained for both electron and gamma irradiation. First, we see that irradiation at 100 Gy has no impact on the ${}^2F_{5/2}$ lifetime in glasses with high or low Yb^{3+} cluster content. The first effect can be seen at 1000 Gy. This result is meaningful for space applications where cumulated doses reach 300 Gy in 10 years, although the dose rate is much lower than the one used in our experiments. Consequently a direct extrapolation of this result to space application is not straightforward.

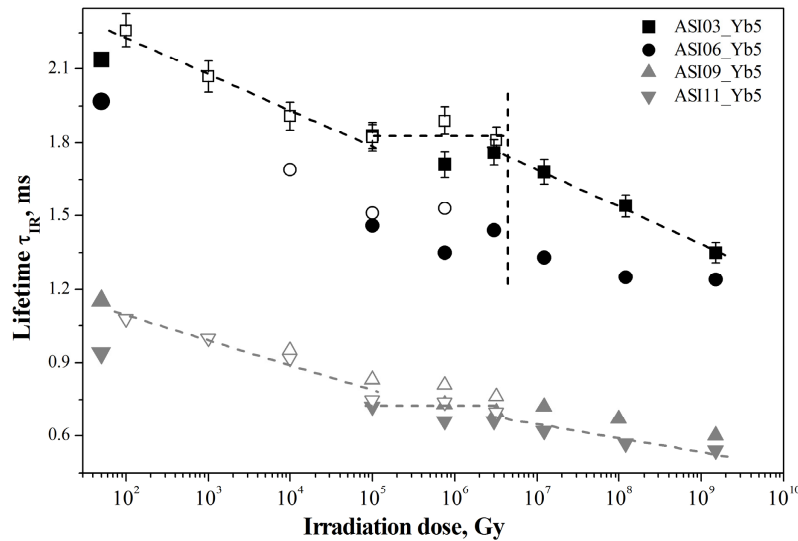


Fig. 5. ${}^2F_{5/2}$ lifetimes for e^- and γ irradiated Yb^{3+} -doped aluminosilicate glasses (measured 6 months after irradiation). Solid (open) symbols: electron (gamma) irradiation; larger symbols: non-irradiated values. Error bars are shown for ASI03_Yb5 glasses only for easier reading.

For glasses with lower ASI parameters – ASI03_Yb5 and ASI06_Yb5 – in both the lower dose range ($<10^5\text{Gy}$) and in the higher dose range ($>3\cdot 10^6\text{Gy}$) clear linear decrease is seen (Fig. 5). However, little or no variation occurs in the $10^5\text{--}3\cdot 10^6\text{Gy}$ dose range. In contrast, for the other two glass compositions with higher ASI parameter, the linear variation in lifetime τ_{IR} presents smaller slopes in the lower and stronger doses regions and there is little evidence for a plateau in the $10^5\text{--}3\cdot 10^6\text{Gy}$ dose range.

We also observed no difference in lifetimes between e^- and γ -irradiated glasses (Fig. 5). This indicates that the concentration and nature of the defects involved in ${}^2F_{5/2}$ quenching are similar in both cases, in the limit of our observations (three dose levels).

The τ_{IR} lifetime evolution was further analyzed in ASI09 aluminosilicate glasses doped with various Yb^{3+} concentrations: 0.5, 5 and 8 wt. % (Fig. 6). At low Yb^{3+} concentration, the behavior of low clustering glasses ASI03 and ASI06 is reproduced, whereas at high Yb^{3+} concentration, the lifetime evolution follows that of ASI09 and ASI011. Taking into account that we checked that clustering is increasing with increasing Yb^{3+} concentration, we conclude that Yb^{3+} clustering, and not glass composition, modifies the evolution of τ_{IR} as a function of irradiation dose.

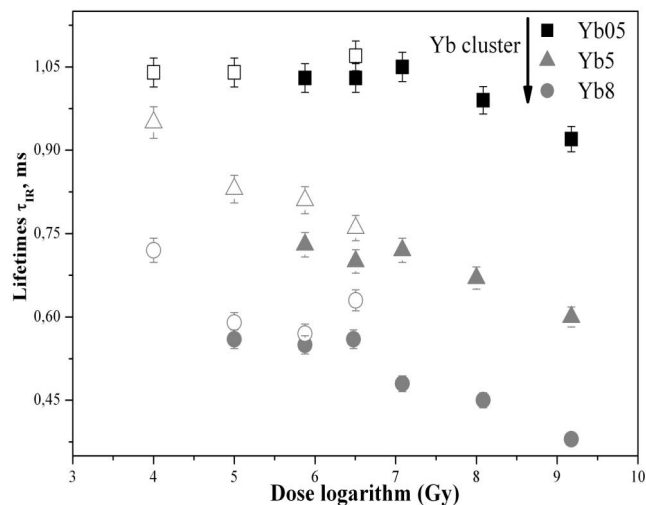


Fig. 6. Variation of the ${}^2F_{5/2}$ decay time value of Yb^{3+} as a function of the logarithmic dose. The irradiation has been performed with e^- -on aluminosilicate glasses ASI09_Ybx with different Yb concentration. Empty symbols are used for gamma irradiation

3.1.3 Correlation between ${}^2F_{5/2}$ lifetime and radiation-induced point defects

In order to understand the ${}^2F_{5/2}$ lifetime variation, we measured the paramagnetic point defects nature and concentration, and their evolution under an annealing treatment. Figure 7 displays the total amount of paramagnetic point defects as a function of irradiation dose. This was determined from double integration of the EPR spectra in the $g = 2$ region [9]. A plateau (10^5 - $3 \cdot 10^6$ Gy) is followed by an increase of defects with increasing dose, and then further followed by a decrease at the highest radiation exposure level. Moreover, glasses with the higher cluster content (ASI09_Yb5 and ASI11_Yb5) show a smaller variation of defects concentration with dose. This is in qualitative agreement with the limited ${}^2F_{5/2}$ lifetime variation with irradiation dose (Fig. 5). For glasses with lower clustering (ASI03_Yb5 and ASI06_Yb5), a similar correlation is observed.

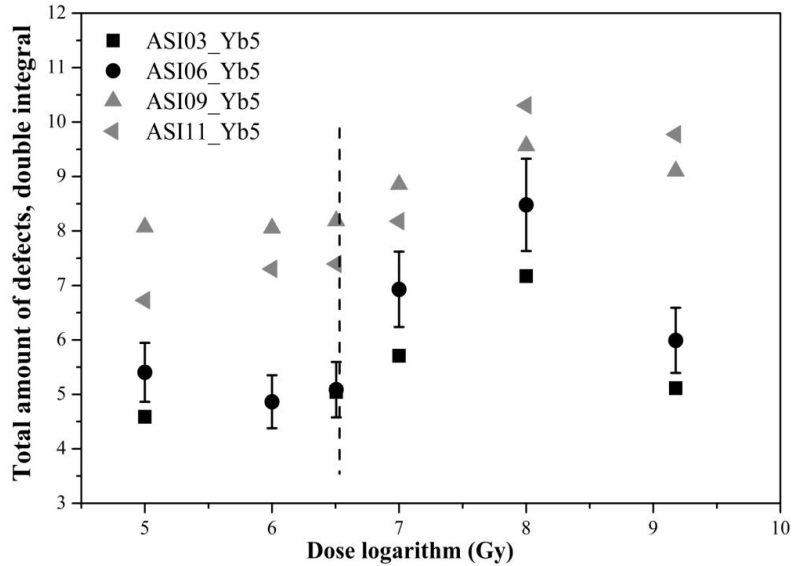


Fig. 7. Total amount of paramagnetic point defects in irradiated Yb^{3+} -doped aluminosilicate glasses.

In order to examine the possible role of particular point defects in lifetime decrease, we carried out annealing treatments on two Yb^{3+} -doped aluminosilicate glasses with opposite Yb^{3+} cluster content: ASI03_Yb5 and ASI09_Yb5. As a matter of fact, bleaching temperature is unique for each defect since it is associated to its energy activation, so an annealing treatment is a tool to separate defect contribution.

The total defect concentration of two Yb^{3+} -doped aluminosilicate glasses as a function of annealing temperatures is presented in Fig. 8. The precise analysis of paramagnetic defect in those glasses was reported in details elsewhere [9]. In ASI03_Yb5, the lifetime of Yb^{3+} excited state ${}^2\text{F}_{5/2}$ is already back to its pre-irradiation value ~ 2.14 ms after annealing at 244°C [Fig. 8(b)]. However, there are still defects in the glass, which are partly identified as HC type (HC1 and HC2) from the EPR spectrum [9]. Moreover, at the same temperature, we observed under 532 nm laser excitation, a broad band centered at 725 nm that we attribute to NBOHC [Fig. 8(b)]. Even if the position is deviated from 620 nm as in SiO_2 glass [13], we assume that the presence of Al can lead a red-shift the position band [14]. We conclude from these results that neither HC defects nor NBOHC defects are solely responsible for the decrease of the ${}^2\text{F}_{5/2}$ lifetime.

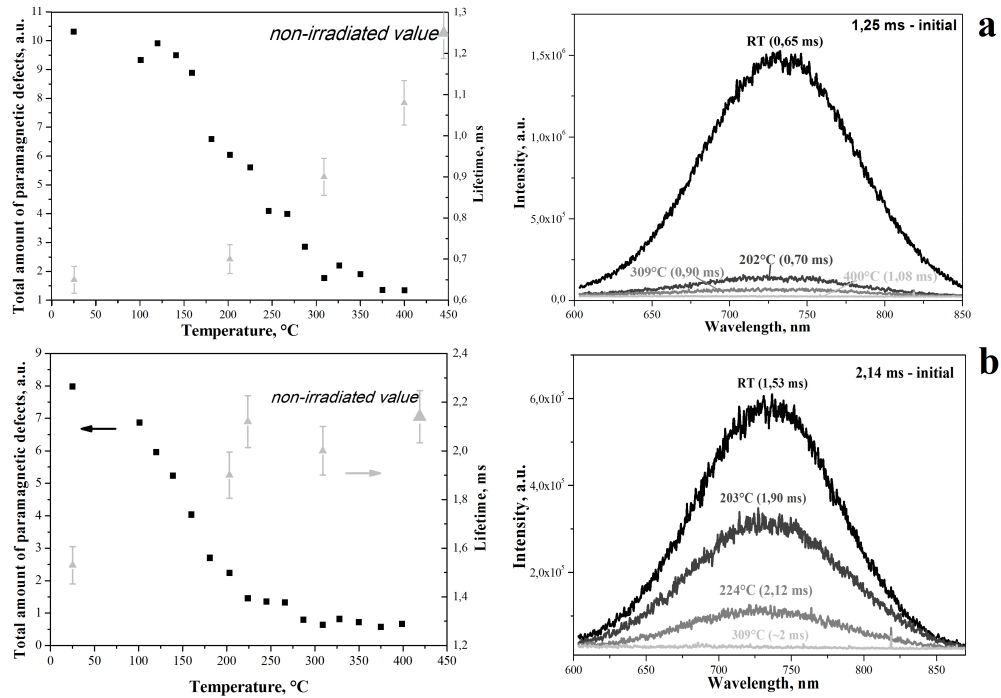


Fig. 8. ${}^2F_{5/2}$ lifetimes and total concentration of paramagnetic defects (left), and photoluminescence spectra of NBOHC (right) in ASI09_Yb5 (a) and ASI03_Yb5 (b) glasses obtained after annealing at various temperatures. Electron irradiation at 10^8 Gy.

Contrary to ASI03_Yb5, τ_{IR} in ASI09_Yb5 is not back to the pre-irradiation value after annealing at 400°C [Fig. 8(a)]. At this temperature, peroxy radicals were evidenced by EPR, whereas neither Al-OHC nor NBOHC defects were detected [Fig. 8(b)]. As the absorption band of peroxy radicals centered at 1.97 eV (630 nm) [13] extends to Yb^{3+} emission range, they could be responsible for the decrease of ${}^2F_{5/2}$ lifetime.

3.2 Extension to other systems

We first studied ${}^2F_{5/2}$ lifetime as a function of irradiation dose and cluster content in Yb^{3+} doped phosphate glasses. As in aluminosilicate glasses, one can observe a multi-step τ_{IR} variation in poly-phosphate glasses, in which the cluster amount is low (Fig. 9), opposed to a monotonically decrease in meta-phosphate glasses with higher Yb^{3+} clustering. The cluster concentration was determined by cooperative luminescence [2]. This result on phosphate glasses first confirms the role of clusters and second suggests that lifetime behavior is irrelevant to the glass composition and consequently on the type of point defect formed.

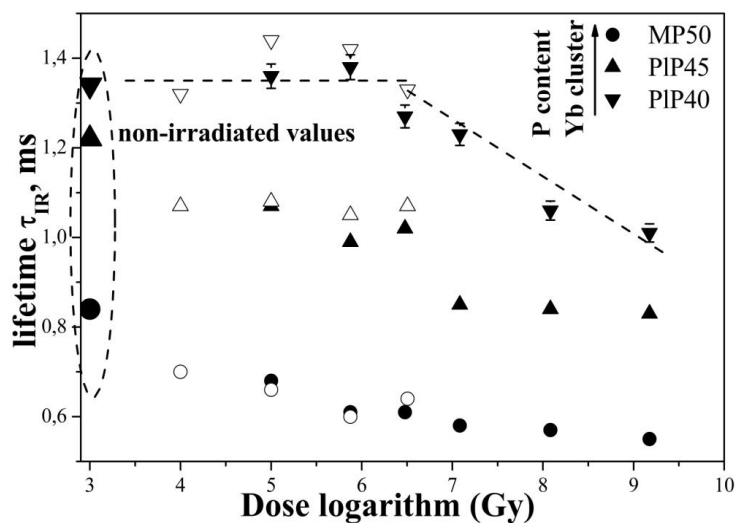


Fig. 9. ${}^2F_{5/2}$ lifetimes of Yb^{3+} doped-phosphate glasses.

We also investigated Er^{3+} doped glasses, in order to further assess the role of clusters. Figure 10 displays the lifetime of ${}^4I_{13/2}$ excited state in ASI03 and ASI09 glasses as a function of $\lg(\text{dose})$. In ASI03_Er05 glass with low Er^{3+} cluster content, the ${}^4I_{13/2}$ lifetime evolution is similar to that of glasses with low Yb^{3+} cluster content, whereas in ASI09_Er05 glass the lifetime variation is lower, as in high Yb^{3+} clustering glasses (see Fig. 5). This suggests that the de-excitation channels via point defect formation are similar for Yb^{3+} and Er^{3+} ions.

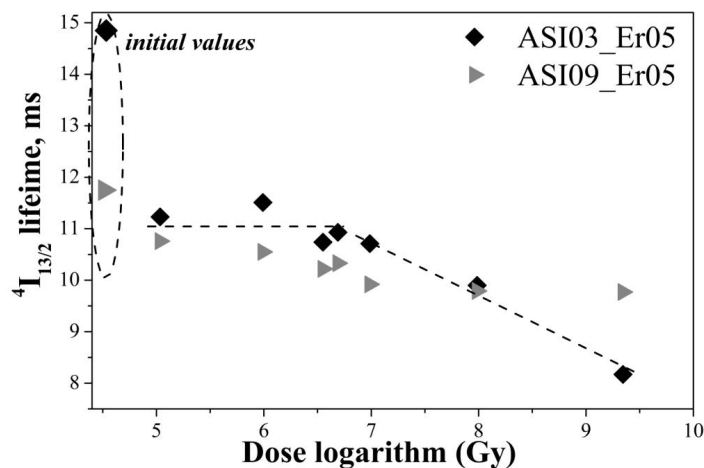


Fig. 10. ${}^4I_{13/2}$ lifetimes of Er^{3+} doped-aluminosilicate glasses.

4. Conclusion

We have studied Yb^{3+} doped aluminosilicate glasses with varying clusters content, which was evidenced by cooperative luminescence and EPR spectroscopy. Yb^{3+} excited state lifetime was recorded as a function of irradiation dose in a 10^2 - $1.5 \cdot 10^9$ Gy range (electron and γ rays) and delays after a 10^5 Gy dose irradiation. Ionizing radiations were found to decrease lifetimes with rates depending primarily on Yb^{3+} clustering and not glass composition. In particular, glasses with high clustering show a smaller decrease in lifetime with increasing radiation dose. This behavior was in agreement with the variation in paramagnetic defects

concentration. The nature of quenching defects was studied by annealing, suggesting that peroxy radicals could have a larger effect than other types of hole centers. In addition, clustering was found to impact lifetimes in Yb³⁺ doped phosphate glasses as well as in Er³⁺ doped aluminosilicate ones. This suggests that this effect could be observed in a broad range of rare earth doped glasses.

Acknowledgments

We thank B. Boizot and V. Metayer for electron irradiations (LSI, SIRIUS, France). The SIRIUS accelerator is a part of National Network of Accelerators Dedicated to Materials Irradiation. We acknowledge A. Mejri for gamma irradiations (Tunisia) and P. Aschehoug (ENSCP, France) for Er and Yb lifetime measurements. We are grateful to F. Tromprier (IRSN, France) for lower dose gamma-irradiations.